

## Magnetic Measurement Results of Tevatron Electron Lens

A.Andriischin, A.Baluyev, S.Kozub, N.Krotov, A.Olyunin, V.Sytnik, A.Tikhov, L.Tkachenko

Institute for High Energy Physics (IHEP), Protvino, Moscow region, 142281 Russia

K.Bishofberger,

University of California at Los Angeles, P.O. Box 951547, Los Angeles, CA 90095-1547

V.Shiltsev

Fermi National Accelerator Laboratory (Fermilab), P.O. Box 500, Batavia, IL 60510-0500

N.Solyak

Branch of Institute Nuclear Physics, Protvino, Moscow region, 142281 Russia

### Introduction

The magnetic system of the Tevatron Electron Lens [1] has strict requirements for longitudinal field quality in its superconducting solenoid. In particular, the deviation of the field lines from a straight line must be less than 0.2 mm along the 1.5-meter central portion of the magnet. These specifications force the magnetic field to be measured with an accuracy of  $10^{-4}$ . Two field-measuring systems have been constructed and used successfully. The first uses a 3D Hall probe, which simultaneously records the field in every direction for each position. The second method is developed to track field lines and is based on the alignment of a magnetic rod along the field and detection of its angle from the axis. This article presents a short description of the measuring equipment and the main results of each measurement.

### 1. Description of magnetic measurement equipment

The block diagram of the 3D Hall probe system is illustrated in Figure 1. A moveable rod supports the Hall probe, which can be translated 240 mm horizontally and 70 mm vertically. Additional rods can be interchanged to offer 1500 mm full range along the z-axis. The spatial resolution of any point is  $10\ \mu\text{m}$  in each direction. Power drivers operate three stepper motors that move the probe, and position sensors provide feedback to the controller mechanism. The direct-control module translates this information into command signals for the motor drivers.

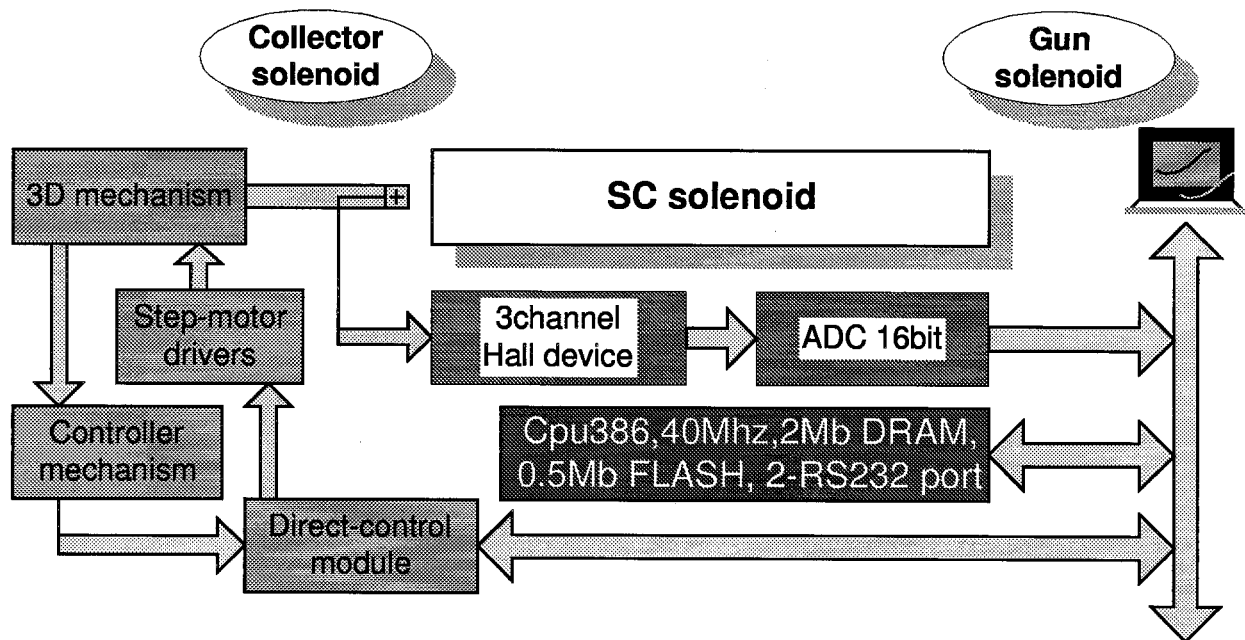
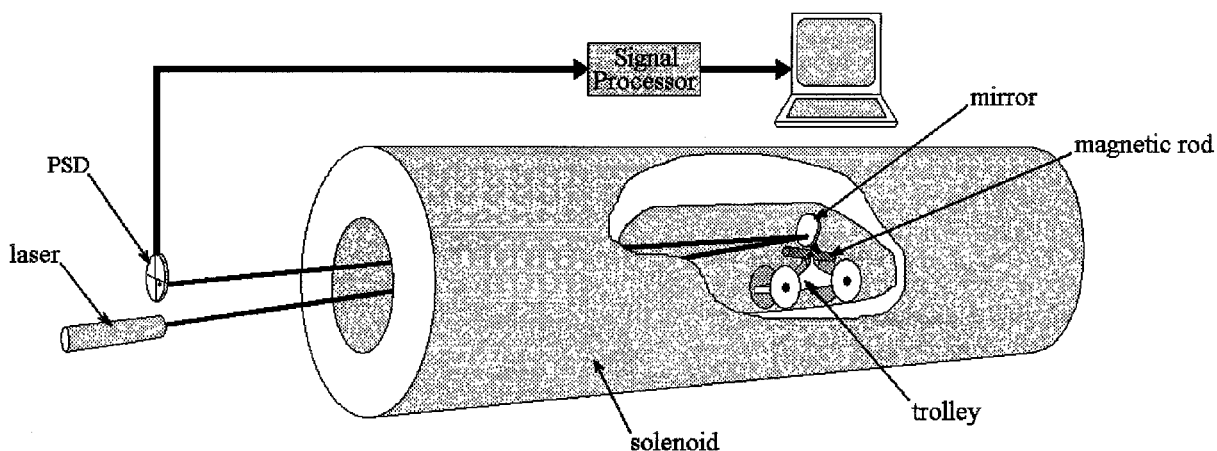


Figure 1. Block diagram of the 3D Hall measurement system.

The analog signals from the 3D Hall probe go to the three-channel Hall device and then to an analogue digital converter (ADC). The digital modules communicate via the data bus to the RS-232 port of a computer. The computer code, written in LabVIEW, is able to measure field data at a single point, along a straight line, along a magnetic line, and throughout a preset area or volume in the Cartesian or cylindrical coordinate systems.

Figure 2 shows a schematic of how the field lines of the superconducting solenoid were measured by the second method. A small trolley holds a freely rotating magnetic rod, and this trolley is moved inside the solenoid by means of a long track. A mirror is glued to the rod and, therefore, also rotates as the rod aligns itself with the local magnetic field. Beyond one end of the solenoid is a small laser aligned along the axis of the trolley's motion. The output beam hits the mirror and reflects back onto a position-sensitive device (PSD). Everything is adjusted so that, at the center of the solenoid, the laser beam is centered on the PSD. As the trolley is moved along the length of the solenoid, small deviations in the magnetic field appear as changes in the location of the reflected laser beam, which are detected by the PSD. The PSD produces signals that are easily converted back to horizontal and vertical displacement of the beam. Through geometry, the angle of the field is deduced, which is integrated to find the transverse displacement of the field along the length of the solenoid. Another LabVIEW program automates the data collection and analysis process. The estimated errors of the spatial resolution are 10  $\mu\text{m}$  vertically and horizontally and 2 mm along the z-axis.



**Figure 2. Schematic drawing of the process to trace the magnetic field lines in the main solenoid. The actual trolley supports a small rod-mirror assembly in a compound gimbal.**

## 2. Conventional solenoids and corrector coils

The collector solenoid has a 20-mm iron cylindrical shield and a 37-mm iron outside cover; the gun solenoid has similar features of 12-mm and 20-mm thickness respectively. The thicker yoke increases the transfer function  $B/I$  and reduces saturation effects (Figure 3, left).

The ellipticity  $\epsilon = 1 - B_y/B_x$  of the magnetic field in the solenoids was measured to be less than  $\pm 0.2\%$ , the accuracy of the measurement system. A corrector coil built into each solenoid can be configured as two dipoles (horizontal and vertical) with 19 G/A field strength of each or as a quadrupole with 6 G/cm/A strength. The corrector magnetic length,

$$L_m = \frac{1}{B_0} \int_{-\infty}^{\infty} B(0,0,z) dz = \frac{1}{G_0} \int_{-\infty}^{\infty} G(0,0,z) dz,$$

was calculated to be 248 mm, making the integrated dipole field equal to 471.2 G-cm/A and the integrated quadrupole field equal to 148.8 G/A. This last value allows one to adjust the ellipticity by 10% at the maximum operating field of 0.4 T. The dipole correctors can rotate the field lines about  $\pm 1.3^\circ$  at the maximum field, which provides  $\pm 10$ -mm displacement of the field lines at the edges of the solenoid.

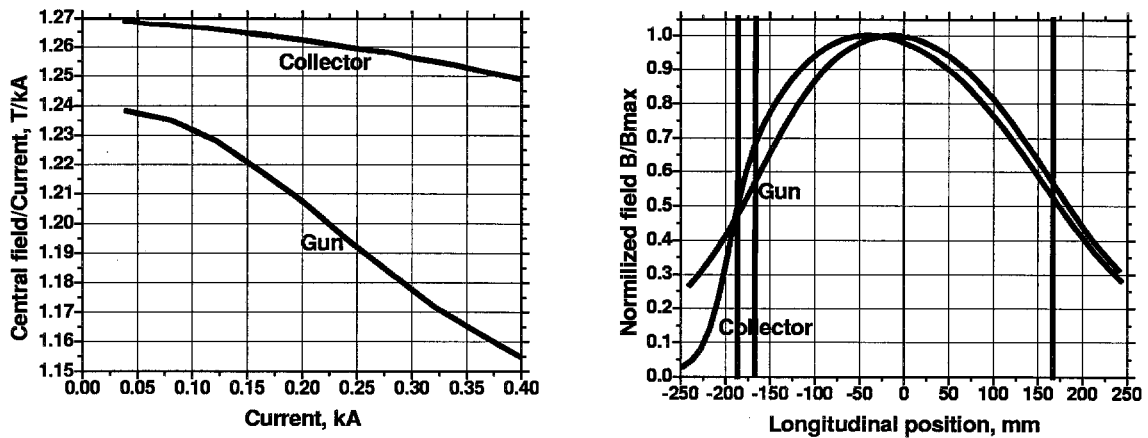


Figure 3. Transfer functions of warm solenoids (left) and distributions of the normalized field along longitudinal axes of warm solenoids (right).

The on-axis residual field along the magnetic axis is approximately 6 G near the iron cover and decreases linearly to about 2 G near the stainless steel cover. The normalized magnetic field strength  $B/B_{max}$  is presented in Figure 3 (right). The center of the coil is defined as  $z = 0$ , and the vertical lines show the length of each solenoid (including the iron shield).

### 3. Superconducting magnets

The superconducting solenoid sustained 6.6 T maximum field before quenching. After this first quench, the magnet reached 6.7 T without quenching. Since this was already higher than the maximum operating field, it was decided not to further increase the current. The transfer function  $k = B/I$  was measured to be 3.65 T/kA (with current measurement accurate to 1%); the calculated value is 3.66 T/kA. The longitudinal distribution of the normalized field  $B/B_{max}$  is shown in Figure 4 (left) for the superconducting magnets, where  $B_{max}$  is equal to 6.5 T in the solenoid (thin line), 0.8 T in the short dipoles, and 0.2 T in the long dipoles (thick lines). The left picture of Figure 4 shows the magnetic lines going out the superconducting solenoids ( $0, \pm 5$  mm) to the beginning of the collector solenoid. The left vertical line marks the edge of the superconducting coil; the right vertical line shows the axis of the collector solenoid. The solid magnetic lines are without short dipole field. The dotted lines present the magnetic lines with 100 A current in the short steering dipole, which corresponds to 0.4 T dipole field. The main fields are 6.5 T in the superconducting solenoid and 0.4 T in the collector solenoid. The initial position of calculated line (the lower solid line) has a little shift (5.1 mm instead 5.0 mm).

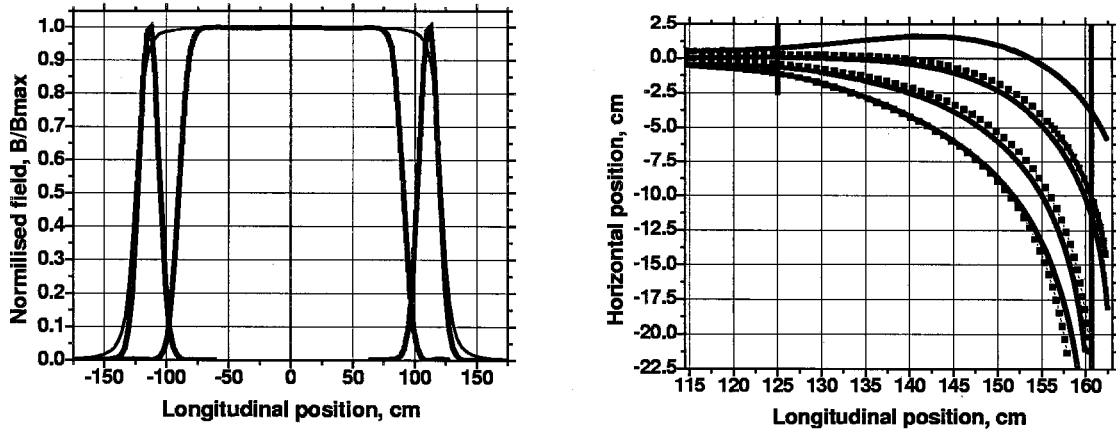


Figure 4. Longitudinal distribution of the normalized fields of the super-conducting magnets (left) and magnetic lines from the superconducting solenoid to the collector one (right).

The deviations of the magnetic axis from a straight line of the superconducting solenoid are shown in Figure 5. At full power, the vertical deviations are very small (roughly spanning  $-25$  to  $25 \mu\text{m}$  of the axis), while the horizontal deviations have more spread (from  $-100$  to  $75 \mu\text{m}$ ); however, these values are still less than the required  $0.2 \text{ mm}$  tolerance. The left side depicts how the field lines change from  $3 \text{ T}$  to  $6 \text{ T}$ , while the right side illustrates how five field lines distributed horizontally differ from each other. The deviations are small enough (about  $8 \mu\text{m}$  maximum, and the horizontal displacement shows similar uniformity) that unintentional lensing effects will be minimal.

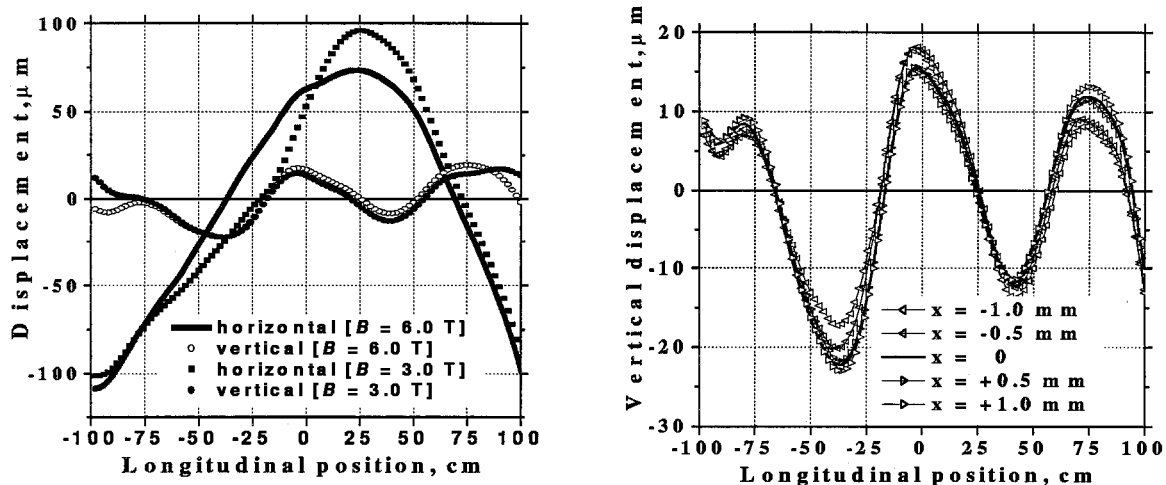


Figure 5.. Transverse displacement of various field lines along the length of the main solenoid, both at different field strengths (left) and at different horizontal positions (right).

## Conclusions

The magnetic characteristics of the Tevatron Electron Lens magnetic system have been measured to high accuracy. All measured results are in good agreement with calculations, and they satisfy the requirements of the TEL. More data is currently being taken to accurately characterize the fields, and when the TEL has been tested, the entire project will be installed in the Tevatron at FNAL.

## References

- [1] I.Bogdanov *et al.* Magnetic system of Tevatron Electron Lens. This Conference.